

# Inhibition of Inter-inverter Harmonic Propagation as a Means to Mitigate Cascaded Commutation Failures in Multi-Infeed LCC-HVdc Systems

Jhair S. Acosta<sup>1</sup>, Hao Xiao<sup>2</sup>, Aniruddha M. Gole<sup>2</sup>

**Abstract**—Earlier research has identified that the phenomenon of cascaded commutation failure (CF) in multi-infeed LCC-HVdc systems connected into weak ac grids is not caused merely by ac voltage reduction, but also significantly by the presence of low order voltage harmonics. Traditional CF mitigation strategies, such as controller optimization have limited effect in reducing such cascaded CFs. In this paper, we propose a novel approach involving the addition of shunt ac filters tuned to the 2nd and 3rd harmonics to mitigate cascaded CF by inhibiting inter-inverter harmonic propagation. These filters significantly reduce the equivalent impedance magnitudes at the relevant harmonics as seen from the local inverter ac bus to the common receiving end grid. As a result, the current harmonics generated by CF in the local inverter are less likely to propagate to remote inverters via the connecting tie-lines. Electromagnetic transient simulations demonstrate that the proposed scheme substantially reduces the probability of cascaded CF under various fault conditions. Furthermore, it is shown that installing only the 2nd or 3rd harmonic-tuned filter, as done in some previous studies, may inadvertently increase the risk of cascaded CF, underscoring the importance of the proposed filtering scheme which targets multiple low order harmonics.

**Keywords**—Cascaded commutation failure, electromagnetic transient simulation, harmonic propagation, multi-infeed LCC-HVdc system, shunt ac filter.

## I. INTRODUCTION

The line-commutated converter (LCC) has been widely used in HVdc for long-distance bulk power transmission, resulting in multi-infeed systems which have multiple inverters within the common receiving end ac grid [1]–[3]. In such systems, commutation failures (CFs) caused by inverter-side ac faults can be classified as "local" and "cascaded" due to complex inter-inverter interactions [4]–[6]. Local CF is attributed to the magnitude reduction or zero-crossing shift of the fundamental frequency waveform at the local inverter ac bus under close-in faults [7]–[9]. Cascaded CF in remote inverters is more complex as it is triggered by voltage harmonics arising from local CF under weak grid conditions, as reported in our earlier research [10], [11]. Developing effective mitigation strategies for cascaded CF is crucial as it may threaten system stability.

Previous CF mitigation strategies have mainly focused on converter controller optimization and auxiliary device installation. For the former, the rectifier dc current order, e.g., voltage-dependent current order limiter (VDCOL), can be transiently reduced to decrease the commutation overlap [12]–[14]. Meanwhile, the inverter delay firing angle order from the constant extinction angle control loop is immediately diminished to enlarge the commutation margin [15]–[17]. However, these control optimization approaches are ineffective with larger commutation voltage depressions under severe ac faults. This problem can be somewhat resolved by installing additional devices, e.g., reactive power compensators [18]–[20], capacitor-commutated modules [21]–[23], fault current limiters [24]–[26], and 2<sup>nd</sup> or 3<sup>rd</sup> harmonic tuned filters [27], [28]. These installed devices can mitigate local CF in multi-infeed systems but cannot effectively reduce the risk of cascaded CF as the harmonic propagation from local to remote inverter ac buses is not well blocked.

Facing these challenges, this paper proposes a new device installation scheme to address cascaded CF and makes the following contributions:

- *Implementation of Dual Harmonic Shunt Filters:* The proposed mitigation strategy involves the addition of shunt filters tuned to the 2<sup>nd</sup> and 3<sup>rd</sup> harmonics. These filters effectively reduce the equivalent impedance at the specified harmonics from the local inverter AC bus to the common receiving end grid. Consequently, the current harmonics generated by local CF produce fewer voltage harmonics, which are less likely to propagate to remote inverters via the tie-lines. This approach significantly lowers the probability of cascaded CF under various fault conditions.
- *Comparison with Single Harmonic Shunt Filters:* It is shown that previous studies [27], [28] that only use a 2<sup>nd</sup> or 3<sup>rd</sup> harmonic-tuned filter have limited effectiveness, as they can inadvertently increase the risk of cascaded CF under weak grid conditions. This underscores the effectiveness and necessity of the proposed dual-filter scheme.

The remainder of this paper is organized as follows: Section II illustrates the mechanism of the cascaded CF phenomenon in multi-infeed systems. Section III proposes the dual harmonic shunt filters scheme and compares it with previous filter scheme. Finally, Section IV concludes the paper.

This work was supported in part by the Mitacs Elevate Postdoctoral Fellowship Program IT39664 and in part by the Natural Sciences and Engineering Research Council (NSERC) of Canada.

1. Jhair S. Acosta is with Manitoba Hydro International, Winnipeg, MB, Canada (corresponding author e-mail: jacosta@mhi.ca)

2. Hao Xiao and Aniruddha M. Gole are with the Department of Electrical and Computer Engineering, University of Manitoba, Winnipeg R3T 2N2, MB, Canada (e-mail: Hao.Xiao1@umanitoba.ca; Aniruddha.Gole@umanitoba.ca).

Paper submitted to the International Conference on Power Systems Transients (IPST2025) in Guadalajara, Mexico, June 8-12, 2025.

## II. ILLUSTRATION OF CASCADED CF MECHANISM IN MULTI-INFEED SYSTEMS

### A. Introduction of Test System

To investigate the cascaded CF, the dual-infeed LCC-HVdc test system shown in Fig. 1 is modeled in the PSCAD/EMTDC program. This system includes two subsystems configured similarly to the CIGRE HVdc Benchmark Model [29]. Inverters 1 and 2 are interconnected via a tie-line in the 50 Hz common receiving end ac grid, which consists of a 187 km transmission segment modeled with the Frequency Dependent (Phase) Model in series with a 6.36  $\Omega$  resistor. The ac/dc system parameters under rated conditions are detailed in Table I. The power base ( $S_b$ ) is 1000 MW, while the ac and dc voltage bases ( $V_{acb}$  and  $V_{dcb}$ ) are 230 kV and 500 kV, respectively. Note that the shunt filters at both inverter ac buses are tuned to the 3.7<sup>th</sup> and 10.7<sup>th</sup> harmonics.

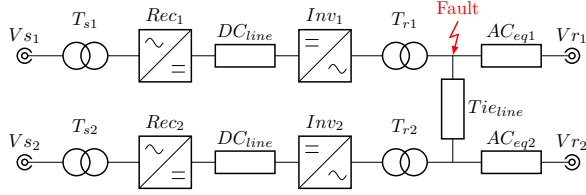


Figure 1. Simplified schematic diagram of dual-infeed test system.

Table I  
MULTI-INFEED TEST SYSTEM CHARACTERISTICS CONSIDERING AN OPERATION FREQUENCY OF 50 HZ.

Converters		
	Rectifier	Inverter
Power (MW)	1000	1000
dc Voltage (kV)	500	500
Firing/extinction angle order (°)	$\alpha = 15$	$\gamma = 15$
Minimum extinction angle (°)		7.2
Shunt Filters		
Apparent power (MVA)	106.88	
Harmonic Filters		
Tuned at harmonic	3.70 <sup>th</sup>	10.70 <sup>th</sup>
Apparent power (MVA)	213.37	215.65
Transformers		
	Rectifier side	Inverter side
Winding voltages (kV)	345/431.14	422.68/230
Apparent power (MVA)	1219.44	1195.53
Positive Leakage reactance (pu)	0.18	0.18
DC Line		
	First half	Second Half
Inductance (H)	0.5968	0.596
Resistance ( $\Omega$ )	2.5	2.5
Capacitance ( $\mu F$ )	26	
AC Systems		
	Rectifier side	Inverter side
SCR	2.5 $\angle 84^\circ$	2.5 $\angle 75^\circ$
Source voltage (kV)	385.52 $\angle 21.32^\circ$	224.48 $\angle -23.35^\circ$
Tie Line modeled as a 187 km TL in series with a R		
Series resistance ( $\Omega$ )	6.36	
TL zero sequence impedance ( $\Omega/m$ )	2.91e-04+j1.16e-03j	
TL +/- sequence impedance ( $\Omega/m$ )	3.43e-05+j4.19e-04j	
TL zero sequence admittance (S/m)	1.88e-09j	
TL +/- sequence admittance (S/m)	2.74e-09j	

### B. Signature of Cascaded CF

To illustrate the phenomenon of cascaded CF, we consider 100 ms ABC-G faults at inverter ac bus 1, as indicated by the

red arrow in Fig. 1. When the fault level exceeds a certain threshold, inverter 1 consistently experiences a local CF. The fault level is defined as the ratio of fault MVA to power base, as shown in Eq. (1), where  $\omega_0$  is the rated ac angular frequency and  $L_f$  is the fault inductance at inverter ac bus 1. A higher fault level corresponds to a smaller  $L_f$ , indicating a more severe fault.

$$FaultLevel = \frac{FaultMVA}{S_b} = \frac{V_{acb}^2 / (\omega_0 L_f)}{S_b} \quad (1)$$

Meanwhile, the impact of the fault level on the probability of CF in remote inverter 2 is shown in Fig. 2. The CF probability is defined as the ratio of fault cases inducing the CF in inverter 2 relative to 100 fault inception instants uniformly distributed over a fundamental frequency cycle. Here, the CF is identified by the differential current criterion in Eq. (2), where the magnitude summation of the three-phase ac currents ( $i_a$ ,  $i_b$ , and  $i_c$ ) flowing from the six-pulse valve group to converter transformer becomes less than two times the dc current  $I_d$  [2]. Based on Eq. (2), Fig. 2 reveals a counter-intuitive probability curve, where a less severe fault (e.g. fault levels of 18.48%) can sometimes exhibit a higher likelihood of the CF in inverter 2 compared to a more severe fault (e.g., fault level of 39.70%). This indicates that the CF in inverter 2 belongs to a "cascaded" type, triggered by the local CF in inverter 1, rather than the fault itself [11]. Typically, the time span from the local to cascaded CF is around 1.5 fundamental frequency cycles [2].

$$|i_a| + |i_b| + |i_c| < 2|I_d| \quad (2)$$

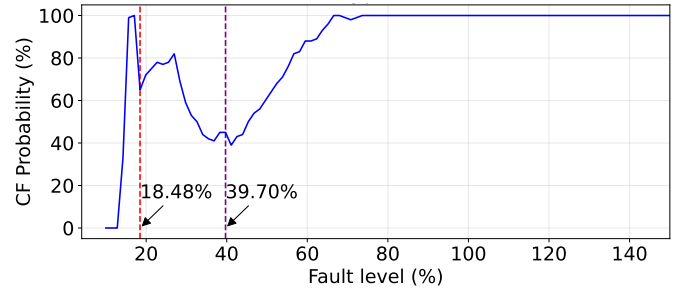


Figure 2. CF probability in remote inverter 2 versus fault level in test system.

### C. Mechanism of Cascaded CF

After inverter 1 experiences a local CF due to the fault, it injects current harmonics into bus 1. This is caused by the asymmetrical operation of the two six-pulse thyristor valve groups and the saturation of the converter transformers. For a less severe fault (e.g., fault level of 18.48%), these current harmonics result in higher voltage harmonics (especially the 2<sup>nd</sup> and 3<sup>rd</sup>) at bus 1 compared to a more severe fault (e.g., 39.70%). This occurs because, at the 18.48% fault level, the equivalent impedance magnitudes at the 2<sup>nd</sup> and 3<sup>rd</sup> harmonics seen from bus 1 to the common receiving end ac grid are larger. Consequently, more voltage harmonics are propagated to remote bus 2 via the tie-line, making inverter 2 more susceptible to cascaded CF.

For illustration, 5 cycle faults, one less severe (18.48% fault level) and the other more severe (39.70% fault level), are simulated at bus 1. It is observed that a cascaded CF at both inverters occurs when the fault is applied at 1.5226 s. However, it is not very meaningful to investigate the harmonics at inverter 2 once it suffers CF, so a fault is applied 1 ms later at 1.5236 s. In this case, CF only occurs at Inverter 1, but it gives us a good idea of harmonic propagation into the inverter 2 ac bus. The response characteristics of 2<sup>nd</sup> and 3<sup>rd</sup> voltage harmonics at bus 2 are presented in Figs. 3 and 4, showing significant increases in voltage harmonics after the local CF for both fault levels. The maximum values of 2<sup>nd</sup> and 3<sup>rd</sup> harmonics during the critical period (from the local CF event to 1.5 fundamental cycles later, highlighted in gray in Figs. 3 and 4) are shown in Table II. The harmonic contents are higher with the less severe 18.48% fault level, despite the higher fundamental component magnitude (88.43%), compared to the more severe fault (84.98%). This indicates that the dip in fundamental voltage is not the primary cause of the cascaded CF. The simulation results suggest that inter-inverter propagation of lower-order harmonics significantly contributes to cascaded CF in the smaller fault level range.

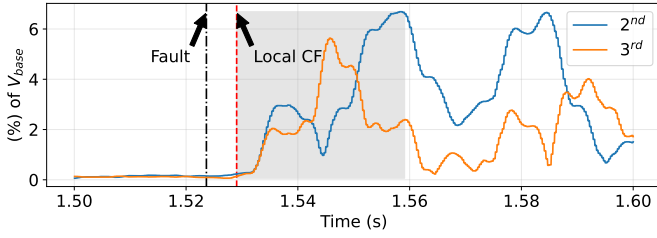


Figure 3. 2<sup>nd</sup> and 3<sup>rd</sup> voltage harmonics at bus 2 for 18.48% fault level.

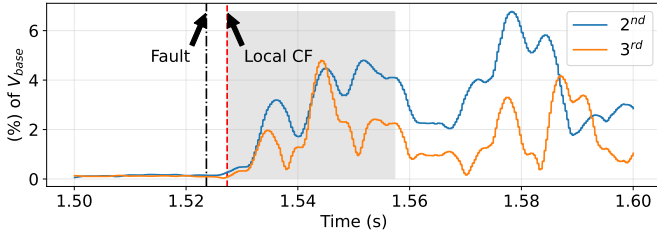


Figure 4. 2<sup>nd</sup> and 3<sup>rd</sup> voltage harmonics at bus 2 for 39.70% fault level.

Table II

COMPARISON OF FUNDAMENTAL VOLTAGE REDUCTION AND HARMONIC COMPONENTS UNDER 18.48% AND 39.70% FAULT LEVELS

Voltage components at bus 2	Fault level	
	18.48%	39.70%
Fundamental frequency voltage magnitude (%)	88.43	84.98
2 <sup>nd</sup> harmonic voltage magnitude (%)	6.69	4.80
3 <sup>rd</sup> harmonic voltage magnitude(%)	5.63	4.79

### III. PROPOSED CASCADED CF MITIGATION STRATEGY IN MULTI-INEED SYSTEMS

#### A. Basic Principle

After inverter 1 experiences a local CF due to the close-in fault, it injects harmonics  $I_{i1}(k)$ ,  $k = 1, 2, \dots, n$  into bus 1.

As the CF is primarily affected by the lower-order harmonics, the 2<sup>nd</sup> and 3<sup>rd</sup> [11] are of most interest. The corresponding voltage harmonic  $V_{i1}(k)$  generated by the current harmonics can be derived by developing the equivalent circuit of the  $k^{th}$  harmonic, as shown in Fig. 5. In this figure,  $z_{c1}(k)$  and  $z_{c2}(k)$  represent the equivalent impedances of the reactive power compensators attached at the inverter ac bus for the  $k^{th}$  harmonic,  $z_{ac1}(k)$  and  $z_{ac2}(k)$  are the equivalent impedances of the ac subgrids at the  $k^{th}$  harmonic,  $z_{tie}(k)$  is the tie-line impedance at the  $k^{th}$  harmonic,  $z_{i2}(k)$  is the equivalent  $k^{th}$  harmonic impedance of inverter 2, and  $z_f(k)$  is the  $k^{th}$  harmonic impedance of the fault branch.

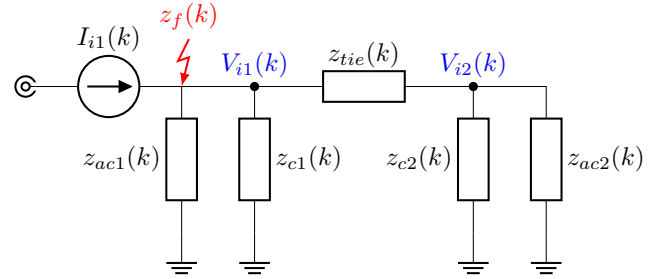


Figure 5. Equivalent circuit of  $k^{th}$  harmonic for cascaded CF analysis.

Referring to Fig. 5, the equivalent  $k^{th}$  harmonic impedance  $z_{eq1}(k)$  looking from bus 1 into the common receiving end ac grid is expressed as shown in Eq. (3).

$$z_{eq1}(k) = [z_{i2}(k) || z_{c2}(k) || z_{ac2}(k) + z_{tie}(k)] || z_{c1}(k) || z_f(k) || z_{ac1}(k) \quad (3)$$

From which,  $V_{i1}(k)$  is computed as shown in Eq. (4).

$$V_{i1}(k) = z_{eq1}(k) I_{i1}(k) \quad (4)$$

$V_{i1}(k)$  after being propagated via the tie-line yields the  $k^{th}$  voltage harmonic at bus 2  $V_{i2}(k)$  as in (5).

$$V_{i2}(k) = V_{i1}(k) \frac{z_{i2}(k) || z_{c2}(k) || z_{ac2}(k)}{[z_{i2}(k) || z_{c2}(k) || z_{ac2}(k) + z_{tie}(k)]} \quad (5)$$

In this paper, the proposed strategy for the cascaded CF mitigation consists in adding shunt filters tuned to the 2<sup>nd</sup> and 3<sup>rd</sup> harmonics at inverter ac buses. With these shunt filters, the magnitudes of  $z_{c1}(k)$  at the 2<sup>nd</sup> and 3<sup>rd</sup> harmonics will both be significantly reduced. Hence,  $z_{eq1}(k)$  is also decreased and  $I_{i1}(k)$  will generate much fewer  $V_{i1}(k)$  according to Eqs. (3) and (4). Further, the magnitude reductions of  $z_{c2}(k)$  at the 2<sup>nd</sup> and 3<sup>rd</sup> harmonics indicate smaller  $V_{i2}(k)$ . As a result of this strategy, the probability of cascaded CF in remote inverter 2 is expected to be lower.

Some previous studies [27], [28] have reported that use of a 2<sup>nd</sup> or a 3<sup>rd</sup> harmonic-tuned filter could reduce the possibility of CF. In this paper, we show that such an approach would decrease the magnitude of  $z_{eq1}(k)$  at the tuned harmonic frequency (e.g.,  $k = 2$  or  $k = 3$ ) and may exhibit unexpected amplifications at the other low order harmonics. For example, a single 3<sup>rd</sup> harmonic-tuned filter may cause

the magnitude of  $z_{eq1}(k)$  to be higher at the  $2^{nd}$  harmonic. As a result, the local CF will cause less  $3^{rd}$  but much more  $2^{nd}$  harmonic distortion. Consequently, the resulting available commutation-voltage integral area [2] for inverter 2 may decrease to a level even below that before the filter was installed, consequently resulting in an increased CF risk. The above challenge faced by previous strategies underscores the effectiveness and necessity of the proposed dual-filter scheme.

### B. Illustration of Harmonic Propagation Inhibition

1) *Proposed dual-harmonic shunt filters:* In order to minimize the filter impact, shunt filters tuned to the  $2^{nd}$  and  $3^{rd}$  harmonic are proposed to replace part of the original shunt compensation in the CIGRE HVdc Benchmark based model at the converter terminals. The proposed  $2^{nd}$  and  $3^{rd}$  harmonic shunt filters have exactly the same MVar rating as the compensation arrangement they replace, namely 106.87 and 215.62 MVA respectively. Thus, the fundamental frequency load flow remains unaffected. The impedance magnitude-frequency characteristics of the proposed filters and original Multi-infeed system are provided in Fig. 6 by the frequency scanning technique. It is seen that the proposed filters exhibit much lower impedance magnitudes at the  $2^{nd}$  and  $3^{rd}$  harmonic frequencies.

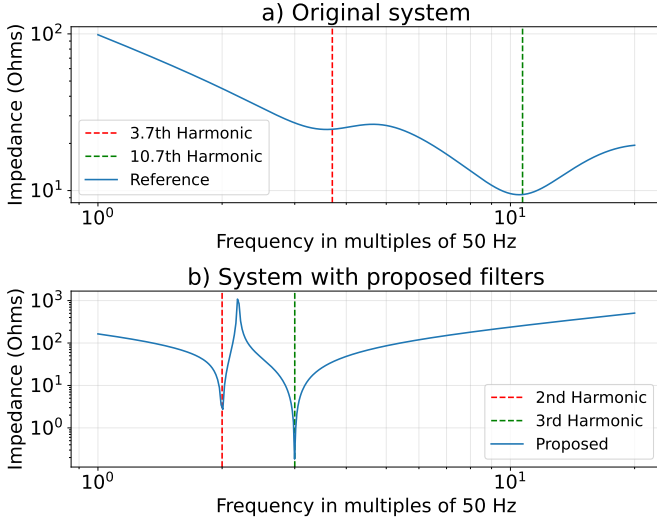


Figure 6. Comparison of impedance magnitude-frequency characteristics between proposed filters and original reference.

#### 2) Impact of proposed filters on harmonic propagation:

The proposed filters are equipped at inverter ac buses 1 and 2 in the test system. To understand how the proposed filters affect the harmonic propagation from bus 1 to 2, a 100 ms fault with fault level at bus 1 of 18.48% is applied at  $t = 1.5236$  s. Note that for this fault case, no cascaded CF is observed in inverter 2. However, this is a threshold case, as even a fractionally earlier fault instant (e.g., 1 ms prior) causes commutation failure. Thus we can say that the measured harmonics for this case would reflect the harmonic scenario when the system is on the verge of CF. The plots of the time variation of  $2^{nd}$  and  $3^{rd}$  voltage harmonics at bus 2 are shown in Fig. 7. Compared to Fig. 3, the  $2^{nd}$  and

$3^{rd}$  voltage harmonics are much reduced than in the original model without filters. For clarity, the maximum values of these harmonics for the time of interest (identified by gray area in Fig. 7) in the cascaded CF analysis are given in Table III. These results hence prove that the proposed filters can well inhibit the harmonic propagation between inverter ac buses 1 and 2.

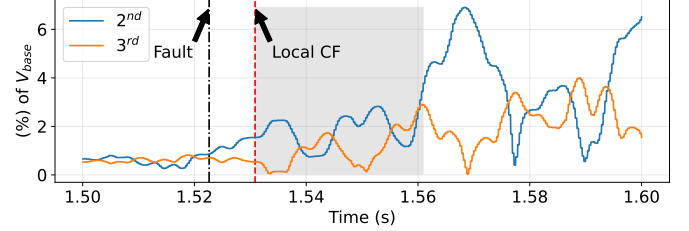


Figure 7. Response characteristics of  $2^{nd}$  and  $3^{rd}$  voltage harmonics at bus 2 for 18.48% fault level with proposed filters.

3) *Comparison with previous strategies:* Previous strategies [27], [28] consist in using only the  $2^{nd}$  or  $3^{rd}$  harmonic-tuned filter. These singly tuned filters are designed to replace the original  $3.7^{th}$  harmonic tuned filter at the inverter ac bus in the CIGRE HVdc Benchmark Model with the same apparent power (215.62 MVA). For comparison with the proposed filters, the previous singly-tuned filters are attached at inverter ac buses 1 and 2 in the test system. The 100 ms fault under 18.48% fault level at bus 1 is simulated at the fault inception instant of 1.5236 s. The maximum values of the plotted harmonics for the time of interest in the cascaded CF analysis are given in Table III.

Table III  
COMPARISON OF HARMONIC PROPAGATION BETWEEN PROPOSED FILTERS AND ORIGINAL REFERENCE

Voltage components at bus 2	$2^{nd}$ harmonic (%)	$3^{rd}$ harmonic (%)
System with proposed strategy	3.98	2.87
Original system	6.69	5.63
Only $2^{nd}$ harmonic filter	12.84	19.23
Only $3^{rd}$ harmonic filter	16.07	16.07

Unlike the same fault scenario with the proposed filters or original reference where no cascaded CF has been observed, previous strategies using either the  $2^{nd}$  or  $3^{rd}$  harmonic-tuned filter trigger the cascaded CF in inverter 2. It can thus be inferred that the proposed filters can block the inter-inverter harmonics and prevent cascaded CF.

### C. Illustration of Cascaded CF Mitigation

1) *Active harmonic-current injection analysis:* In Section III-B, the harmonic propagation has shown to be inhibited by the proposed filters. How to quantify the impact of this inhibition on the cascaded CF in inverter 2 will be further studied here. As the cascaded CF originates from the current harmonic injection at bus 1 due to the local CF in inverter 1, harmonic currents can be actively injected at bus 1 to assess the role of the harmonic propagation attenuation. If a larger amount of harmonic content is required to induce the cascaded

CF, the harmonic propagation is more blocked and thus less likely to affect the operation of inverter 2.

For the system with the proposed filters and the original system, the impact of the harmonic injection values on the occurrence of the cascaded CF is presented in Figs. 8 and 9 respectively. As per the above active harmonic-current injection scheme,  $2^{nd}$  and  $3^{rd}$  harmonics are injected at bus 1 separately and together. Three cases are simulated, i.e., only  $2^{nd}$ , only  $3^{rd}$  harmonic, and both. From Figs. 8 and 9, it is firstly clear that both the  $2^{nd}$  and  $3^{rd}$  harmonics influence the occurrence of the cascaded CF either in the system with the proposed filters or in the original system. Specifically, the  $2^{nd}$  harmonic has a more substantial impact because smaller values are required to precipitate the cascaded CF. Secondly, the required harmonic-current injection values for all three cases with system of the proposed filters are uniformly higher than original system. Take for example the case of  $3^{rd}$  harmonic injection. In the original system (middle curve in Fig. 8), it takes 1.1% to induce a cascaded CF, whereas with the filters, a much stronger injection of 1.7% is required. The above information thereby indicates that inverter 2 is less prone to the cascaded CF as the harmonic propagation between the two inverters is reduced.

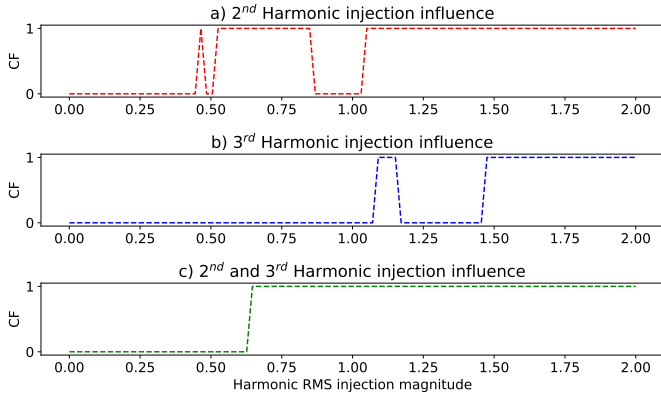


Figure 8. Impact of  $2^{nd}$  and  $3^{rd}$  harmonic-current injection values on cascaded CF with original system.

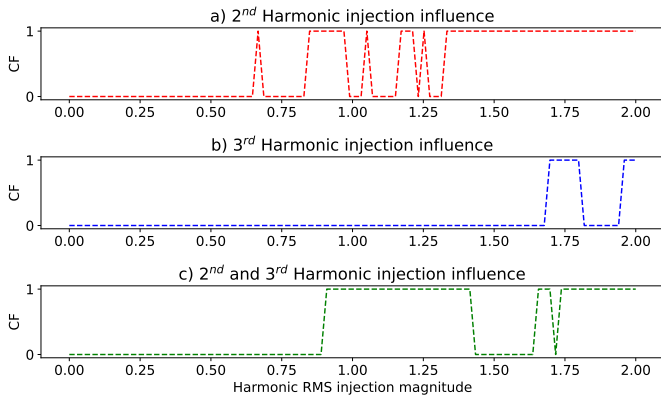


Figure 9. Impact of  $2^{nd}$  and  $3^{rd}$  harmonic-current injection values on cascaded CF for system with proposed filters.

2) *Comparison with previous strategies on cascaded CF probability:* The previous section demonstrates that the proposed filters can inhibit the inter-inverter harmonic propagation. In this section, the probability characteristics of the cascaded CF under the proposed filters and previous strategies will be further explored considering various fault conditions on the test system. For this, one hundred faults were distributed over a period of one cycle of fundamental frequency. Likewise, a hundred fault levels were considered, ranging from 4% to 160%, for each fault type, e.g., A-G, AB-G, and ABC-G fault types, to generate the CF probability curves as shown in Figs. 10 to 12. The interconnecting tie-line between the converter buses is represented by a Frequency Dependent (Phase) Model of the transmission line.

Figs. 10 to 12 all show that the probability of CF is much reduced when both filters are present. Surprisingly, when only one filter (i.e., 2nd or 3rd) is used, as reported in previous approaches, the CF probability becomes even larger than the original system for all three fault types. This indicates that previous approaches may be detrimental to the commutation in inverter 2 under weak ac grid conditions. In summary, the proposed  $2^{nd}$  and  $3^{rd}$  filters can better mitigate the cascaded CF than previous strategies as far as its probability is concerned. The only anomaly is for the A-G fault case, in which the original system shows a lower CF rate than the one with filters for fault levels less than 60%, as shown in Fig. 12.

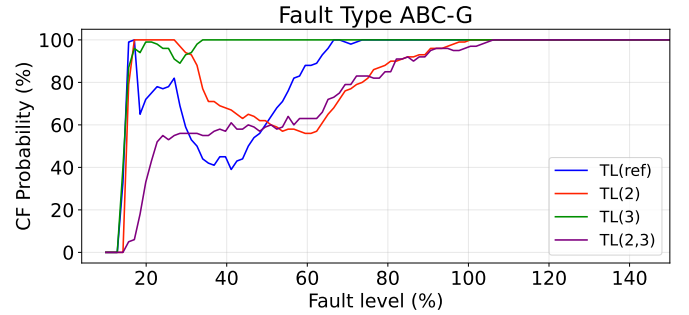


Figure 10. Impact of fault level on cascaded CF probability for ABC-G fault using different filter schemes.

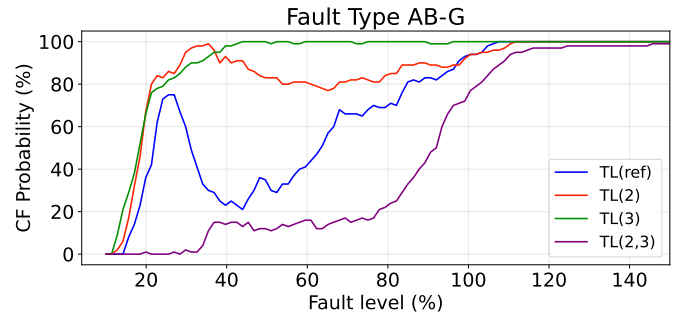


Figure 11. Impact of fault level on cascaded CF probability for AB-G fault using different filter schemes.



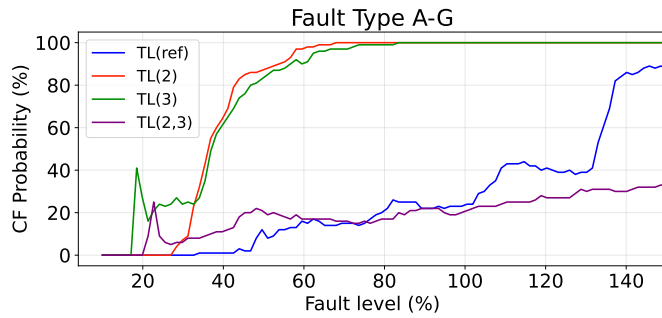


Figure 12. Impact of fault level on cascaded CF probability for A-G fault using different filter schemes.

3) *Impact of ac tie-line representation:* The CF analysis in previous sections has been done using a Frequency Dependent (Phase) Model for the interconnecting ac tie-line. In many studies, it is also common to use the simple resistor-inductor in series (R-L) model in CF investigations [1]–[3]. The efficacy of the proposed filters is further checked by comparing the above two tie-line representations in the test system, both with the same fundamental frequency impedance ( $13.09 + 78.3j \Omega$ ). It is observed that the general trends are the same regardless of the representation used. As an illustration, Fig. 13 shows the CF probabilities for the various filter configurations and original system for AB-G faults when the R-L representation is used. The behaviour is qualitatively identical to that obtained with the frequency domain representation in Fig. 11, although a more closer inspection shows that the transmission line model has a marginally higher commutation failure probability.

Thus, it is clear that with the R-L model, the conclusions made on the comparison of the cascaded CF between the proposed filters and previous strategies are still valid. That is, the proposed filters behave better than previous strategies in decreasing the cascaded CF likelihood.

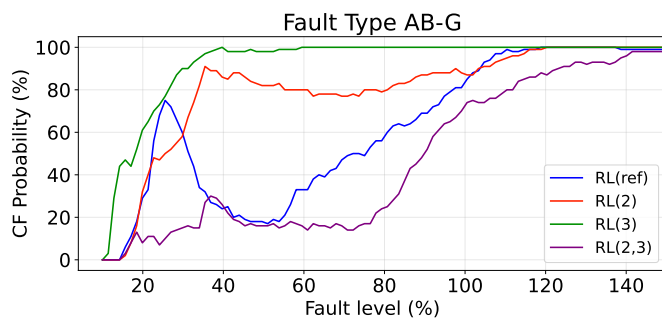


Figure 13. Comparison of transmission line and R-L models on impact of fault level on cascaded CF probability for AB-G fault using different filter schemes.

#### IV. CONCLUSIONS

This paper shows that propagation of lower order harmonics generated at one converter by a local commutation failure can propagate to the other converter creating a Cascaded Commutation failure. This behaviour can be improved with the addition of dual-harmonic shunt filters.

To summarize:

- The proposed filters could effectively reduce the equivalent impedance magnitudes at the 2<sup>nd</sup> and 3<sup>rd</sup> harmonics seen from the inverter ac bus. Hence, the harmonics originating from the local CF would be diminished at the remote inverters, thereby reducing the probability of such cascaded CFs in multi-infeed systems.
- Using only either the 2<sup>nd</sup> or 3<sup>rd</sup> harmonic-tuned filters individually as proposed in previous publications might inadvertently increase the risk of the cascaded CF under weak grid conditions. This further emphasizes the necessity of the proposed filters.
- Representing the ac tie-line by the more accurate transmission line model is recommended in CF analysis in multi-infeed systems. However, using of a simple R-L tie line representation gives qualitatively similar results.
- This work can be extended in the future to design improved filter topologies and determine the optimal filter ratings, quality factors and economical design.

#### REFERENCES

- [1] CIGRE WG B4.41, "Systems with multiple DC infeed," CIGRE working group 364, Tech. Rep. December, 2008.
- [2] H. Xiao, J. S. Acosta, A. M. Gole, X. Duan, and Y. Zhang, "Investigation of cascaded commutation failures in multiple lcc-hvdc inverters caused by rectifier side ac grid faults," *IEEE Transactions on Power Delivery*, vol. 39, no. 4, pp. 2446–2456, 2024.
- [3] N. Chen, Y. Yang, L. Li, C. Cui, Y. Xue, and X.-P. Zhang, "Commutation failure prediction for multi-infeed lcc-hvdc systems under asymmetrical faults," *IEEE Transactions on Power Delivery*, vol. 38, no. 3, pp. 2034–2046, 2023.
- [4] J. S. Acosta, H. Xiao, and A. M. Gole, "Sensitivity analysis of commutation failure in multi-infeed hvdc systems: Exploring the impact of ac system representations and fault types," *ELECTRIC POWER SYSTEMS RESEARCH*, vol. 234, SEP 2024.
- [5] E. Rahimi, A. M. Gole, J. B. Davies, I. T. Fernando, and K. L. Kent, "Commutation failure in single- and multi-infeed HVDC systems," in *8th IEE International Conference on AC and DC Power Transmission (ACDC 2006)*, vol. 2006, no. 1. IEE, 2006, pp. 182–186.
- [6] R. O. Fernandes and M. C. D. Tavares, "Mitigation of the commutation failure problem in the hvdc multi-infeed scenario in brazil using synchronized phasor measurement," *ELECTRIC POWER SYSTEMS RESEARCH*, vol. 235, OCT 2024.
- [7] C. Thio, J. Davies, and K. Kent, "Commutation failures in hvdc transmission systems," *IEEE Transactions on Power Delivery*, vol. 11, no. 2, pp. 946–957, 1996.
- [8] Y. Shao and Y. Tang, "Fast evaluation of commutation failure risk in multi-infeed hvdc systems," *IEEE Transactions on Power Systems*, vol. 33, no. 1, pp. 646–653, 2018.
- [9] H. Xiao, Y. Li, J. Zhu, and X. Duan, "Efficient approach to quantify commutation failure immunity levels in multi-infeed hvdc systems," *IET GENERATION TRANSMISSION & DISTRIBUTION*, vol. 10, no. 4, pp. 1032–1038, MAR 10 2016.
- [10] E. Rahimi, A. M. Gole, J. B. Davies, I. T. Fernando, and K. L. Kent, "Commutation Failure Analysis in Multi-Infeed HVDC Systems," *IEEE Transactions on Power Delivery*, vol. 26, no. 1, pp. 378–384, jan 2011. [Online]. Available: <http://ieeexplore.ieee.org/document/5673966/>
- [11] H. Xiao, Y. Li, A. M. Gole, and X. Duan, "Computationally efficient and accurate approach for commutation failure risk areas identification in multi-infeed lcc-hvdc systems," *IEEE Transactions on Power Electronics*, vol. 35, no. 5, pp. 5238–5253, 2020.
- [12] C. Taylor and S. Lefebvre, "Hvdc controls for system dynamic performance," *IEEE Transactions on Power Systems*, vol. 6, no. 2, pp. 743–752, 1991.
- [13] R. Bunch and D. Kosterev, "Design and implementation of ac voltage dependent current order limiter at pacific hvdc intertie," *IEEE Transactions on Power Delivery*, vol. 15, no. 1, pp. 293–299, 2000.
- [14] J. Wang, M. Huang, C. Fu, H. Li, S. Xu, and X. Li, "A new recovery strategy of hvdc system during ac faults," *IEEE Transactions on Power Delivery*, vol. 34, no. 2, pp. 486–495, 2019.

- [15] S. Tamai, H. Naitoh, F. Ishiguro, M. Sato, K. Yamaji, and N. Honjo, "Fast and predictive hvdc extinction angle control," *IEEE Transactions on Power Systems*, vol. 12, no. 3, pp. 1268–1275, 1997.
- [16] H.-I. Son and H.-M. Kim, "An algorithm for effective mitigation of commutation failure in high-voltage direct-current systems," *IEEE Transactions on Power Delivery*, vol. 31, no. 4, pp. 1437–1446, 2016.
- [17] S. Mirsaeidi, X. Dong, D. Tzelepis, D. M. Said, A. Dyśko, and C. Booth, "A predictive control strategy for mitigation of commutation failure in lcc-based hvdc systems," *IEEE Transactions on Power Electronics*, vol. 34, no. 1, pp. 160–172, 2019.
- [18] R. Hong, X. Shukai, Z. Yong, H. Chao, and W. Wei, "Research and application of multiple statcoms to improve the stability of ac/dc power systems in china southern grid," *IET Generation, Transmission & Distribution*, vol. 10, pp. 3111–3118(7), October 2016.
- [19] Y. Zhang and A. M. Gole, "Quantifying the contribution of dynamic reactive power compensators on system strength at lcc-hvdc converter terminals," *IEEE Transactions on Power Delivery*, vol. 37, no. 1, pp. 449–457, 2022.
- [20] O. Nayak, A. Gole, D. Chapman, and J. Davies, "Dynamic performance of static and synchronous compensators at an hvdc inverter bus in a very weak ac system," *IEEE Transactions on Power Systems*, vol. 9, no. 3, pp. 1350–1358, 1994.
- [21] K. Sadek, M. Pereira, D. Brandt, A. Gole, and A. Daneshpooy, "Capacitor commutated converter circuit configurations for dc transmission," *IEEE Transactions on Power Delivery*, vol. 13, no. 4, pp. 1257–1264, 1998.
- [22] Y. Xue, X.-P. Zhang, and C. Yang, "Commutation failure elimination of lcc hvdc systems using thyristor-based controllable capacitors," *IEEE Transactions on Power Delivery*, vol. 33, no. 3, pp. 1448–1458, 2018.
- [23] C. Guo, Z. Yang, B. Jiang, and C. Zhao, "An evolved capacitor-commutated converter embedded with antiparallel thyristors based dual-directional full-bridge module," *IEEE Transactions on Power Delivery*, vol. 33, no. 2, pp. 928–937, 2018.
- [24] H. Huang, Z. Xu, and X. Lin, "Improving performance of multi-infeed hvdc systems using grid dynamic segmentation technique based on fault current limiters," *IEEE Transactions on Power Systems*, vol. 27, no. 3, pp. 1664–1672, 2012.
- [25] S. Mirsaeidi, X. Dong, and D. M. Said, "A fault current limiting approach for commutation failure prevention in lcc-hvdc transmission systems," *IEEE Transactions on Power Delivery*, vol. 34, no. 5, pp. 2018–2027, 2019.
- [26] H.-J. Lee, G. T. Son, J.-I. Yoo, and J.-W. Park, "Effect of a sfcl on commutation failure in a hvdc system," *IEEE Transactions on Applied Superconductivity*, vol. 23, no. 3, pp. 5 600 104–5 600 104, 2013.
- [27] G. Kristmundsson and D. Carroll, "The effect of ac system frequency spectrum on commutation failure in hvdc inverters," *IEEE Transactions on Power Delivery*, vol. 5, no. 2, pp. 1121–1128, 1990.
- [28] S. Lin, D. Mu, L. Xu, and Z. He, "Parameter optimization method for ac filters in hvdc considering reactive power compensation effectiveness," *IEEE Transactions on Power Delivery*, pp. 1–11, 2024.
- [29] M. Szechtman, T. Wess, and C. Thio, "A benchmark model for hvdc system studies," in *International Conference on AC and DC Power Transmission*, 1991, pp. 374–378.